Self-Amplified Surface Charging and Partitioning of Ionic Liquids in Nanopores

Justin N. Neal,[1] K. L. Van Aken,[2] Y. Gogotsi,[2] David J. Wesolowski,[3] and Jianzhong Wu[1,*]

[1]*Department of Chemical and Environmental Engineering and Applied Mathematics, University of California, Riverside, California 92521, USA*

[2]*Department of Materials Science and Engineering, A.J. Drexel Nanomaterials Institute, Drexel University, Philadelphia, Pennsylvania 19104, USA*

[3]*Chemical Sciences Division, Oak Ridge National Laboratory, Oak Ridge, Tennessee 37831, USA*

(Received 24 August 2016; revised manuscript received 17 May 2017; published 22 September 2017)

We study ion partitioning and self-charging of nanoporous electrodes with room-temperature ionic liquids using a classical density-functional theory that accounts for molecular-excluded volume effects and electrostatic correlations. Nanopores of zero electrical potential are predicted to favor adsorption of small ions even without specific surface attraction, and the imbalanced distributions of cations and anions inside the pore induces a net surface charge that promotes further enrichment of small ions. The self-amplified ion partitioning is most significant when the nanopore and the ionic species are of comparable dimension.

DOI: 10.1103/PhysRevApplied.8.034018

I. INTRODUCTION

Room-temperature ionic liquids (RTILs) are promising to pair with nanoporous electrodes for the next generation of electrochemical devices such as supercapacitors [1], batteries [2], and fuel and solar cells [3]. Good knowledge of ion partitioning into the micropores of the electrodes and the interfacial properties of ionic species is of fundamental importance for both materials design and device optimization. While recent years have witnessed enormous progress in understanding ion interactions with nanopores under various aqueous environments, much less is known about the electrochemical behavior of RTILs inside nanopores [4–7]. In comparison to aqueous electrolytes, RTILs are promising because they allow for the expansion of the voltage window [8] and the range of temperature operation [9] for energy-storage devices. The properties of confined ionic liquids are expected to be drastically different from those corresponding to aqueous or even organic electrolyte solutions due to the lack of solvation, much higher concentrations of ionic species, and stronger pair electrostatic interactions.

An electrode will typically develop a net charge at the surface in the presence of an electrolyte even when its electrical potential is fixed at 0 V by an external circuit (viz., grounded) [10]. The surface charge arises from the asymmetric distribution cations and anions in the interfacial region known as the electric double layer (EDL). As electroneutrality must be satisfied for the entire system, the net charge at the electrode surface is equal in magnitude but opposite in sign to that of the electrolyte. Most electrodes for capacitive energy storage are made of amorphous carbons containing micropores that often have a multimodal or just a broad pore size distribution [11]. Whereas the surface charging of a single planar electrode is intuitive, the situation becomes more complicated if the electrode contains a broad range of micropores. Ion partitioning into the individual pores and the resulting EDL structure depend not only on the intrinsic properties of the ionic species but also on the detailed specifications of the confining space.

For micropores in contact with an aqueous solution, ion partitioning and selectivity have been extensively studied in recent years by both theoretical and experimental means [12–16]. It has been found that a charged micropore enriches counterions over coions due to the electrostatic attraction, and in the presence of mixed counterions of the same valence, it favors the preferential adsorption of smaller counterions due to the stronger surface energy. If the micropore is neutral or dehydrated, larger ions are often preferred inside the pore. For a micropore in contact with mixed ions of different sizes and valences, ion partitioning and selectively reflect a competition of electrostatic interactions and excluded volume effects [17,18]. While much is known about ion selectivity for aqueous systems, we are unaware of previous investigations of ion-partitioning behavior for micropores in equilibrium with RTILs.

In this work, we investigate the selectivity and the partitioning of mixed ionic species from RTILs into the nanopores of carbon electrodes. The electrochemical system mimics what has been studied in a recent experiment for supercapacitors consisting of carbide-derived-carbon (CDC) and ionic liquid mixtures [19]. According to the pore size distribution obtained from gas sorption analysis, the Mo_2C-CDC electrode material consists of two types of nanopores. The average dimensions of small and large pores are 0.8 and 2.67 nm, respectively [20]. Mixed electrolytes are used for supercapacitor applications because cations and anions of the RTILs typically have

*Corresponding author.
jwu@engr.ucr.edu

different electrochemical stability. As a result, the maximum working potentials of the negative and positive electrodes are asymmetric, and such an asymmetry can affect the operational potential window. An ionic liquid mixture is able to expand the electrical potential window by balancing the electrode performance during the supercapacitor charging and discharging. Although the system considered in this work is motivated to improve supercapacitor performance, we believe that the generic physics has a broader implication for understanding ion distributions in nanopores.

II. MOLECULAR MODEL AND METHODS

To capture the salient features of RTILs and nanoporous electrodes, we use a coarse-grained model for the electrochemical system. We represent both cations and anions as charged spheres as in the primitive model of electrolytes and the micropores of the CDC electrode as hard-wall slits. The slit-pore model is commonly used in the experimental characterization of amorphous materials including the CDC considered in this work [21]. In addition, ion confinement between two parallel hard walls represents one of the most popular pore models for the theoretical investigations of EDL and ion distributions in nanopores [22]. The electrical potential at the surface is fixed at zero such that ion partitioning is not biased by an arbitrary attractive energy.

Figure 1 shows a schematic representation of the model ionic system. The pair potential between the ionic species is given by

$$u_{ij}(r) = \begin{cases} \infty, & r < (\sigma_i + \sigma_j)/2, \\ Z_i Z_j e^2/4\pi\varepsilon_0 r, & r \geq (\sigma_i + \sigma_j)/2, \end{cases} \quad (1)$$

where r is the center-to-center distance, e is the elementary charge, ε_0 is the permittivity of free space, and σ_i and Z_i are, respectively, the diameter and the valence of particle i. We use the unity dielectric constant in Eq. (1) because all components in the system are explicitly considered in our model ionic liquid. One should realize that the pair potential is referred to as the Coulomb interaction between two charged particles (here, coarse-grained ions) in vacuum, which has a unity dielectric constant. In other words, the dielectric constant for interaction between two isolated ions is different from that of the bulk ionic system.

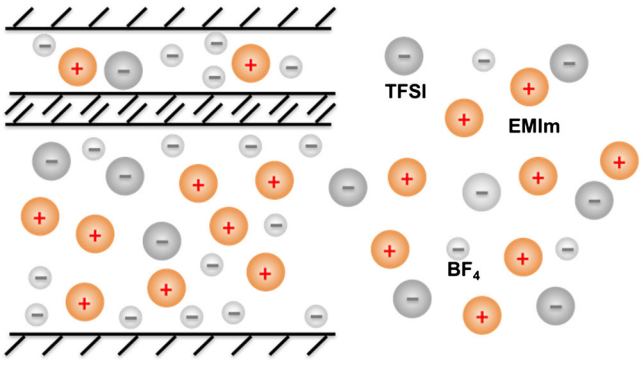

FIG. 1. A schematic representation for ion partitioning between nanopores and a RTIL containing two types of anions of different sizes (TFSI and BF_4) and one type of cation (EMIm).

As in the typical model of electrolytes, we assume that the van der Waals forces, including the surface and ion polarizability effects, are relatively insignificant in comparison with the bare electrostatic interactions between ion pairs in vacuum. It has been shown that the coarse-grained model is able to reproduce the layer-by-layer structure of cations and anions near a charged surface [23], and the pore size dependence of the EDL capacitance in ionic liquid systems is in good agreement with experiments [24]. Although the coarse-grained model lacks the chemical details, it accounts for electrostatic correlations and molecular-excluded volume effects most important for describing the charging behavior of the electrochemical system.

We select the model parameters by matching the molecular volumes and the net charges of three ionic species used in the experimental system: 1-ethyl-3-methylimidazolium (EMIm), bis(trifluoromethylsulfonyl) imide (TFSI), and tetrafluoroborate (BF_4) [19]. The diameter of the cations (EMIm) is fixed at $\sigma_+ = 0.5$ nm, and the diameters of the two anions TFSI and BF_4 are 0.5 and 0.3 nm, respectively. We deliberately use the same diameter for the cations and the large anions because they constitute a symmetric electrolyte system that is often used as a reference. For all ionic mixtures, the overall number density of ionic species in the bulk is fixed at 4.64 nm^{-3}, approximately matching the mass density (1.3 g/ml) of the RTIL mixtures [24].

Within the primitive model of electrolytes, the distribution of cations and anions in a slit pore can be readily predicted from the classical density-functional theory (DFT) [25]. At a given temperature T and a set of ionic number densities in the bulk, ρ_i^0, DFT predicts that the density profiles within the slit pore are given by

$$\rho_i(z) = \rho_i^0 \exp[-\beta V_i(z) - \beta Z_i e\psi(z) - \beta\Delta\mu_i^{\mathrm{ex}}(z)], \quad (2)$$

where z represents the perpendicular distance from a surface of the slit pore, $\beta = 1/(k_B T)$, k_B is the Boltzmann constant, $V_i(z)$ is the external potential confining the ionic species inside the pore, and $\Delta\mu_i^{\mathrm{ex}}(z)$ accounts for the thermodynamic nonideality arising from electrostatic correlations and ionic excluded volume effects [25]. It should be noted that our model does not contain a fixed layer of ions at the surface as in the continuous model of the electric double layer. Each ion is considered explicitly, having a finite size and charge. The entire pore is neutral; i.e., the surface charge is exactly balanced by the net charge of ionic species inside the pore.

The electrical potential $\psi(z)$ is related to the local charge density by the Poisson equation

$$\frac{\partial^2\psi(z)}{\partial z^2} = -\frac{e}{\varepsilon_0}\sum_i Z_i\rho_i(z). \tag{3}$$

Equations (2) and (3) can be solved numerically with the electrical potential at the surface set as zero, i.e., $\psi_s = \psi(0) = (H) = 0$. The analytical expression for $\Delta\mu_i^{\mathrm{ex}}(z)$, and the numerical details for the DFT calculations are reported in our previous publications [26]. It is worth noting that without $\Delta\mu_i^{\mathrm{ex}}(z)$, Eqs. (2) and (3) reduce to the Poisson-Boltzmann equations, which are conventionally used to describe ion distributions in inhomogeneous aqueous systems. Because the surface electrical potential is taken as a constant throughout this work, the electric field inside the pore is exclusively determined by the ionic distributions, immaterial to the electronic properties of the electrode. Whereas the local dielectric inhomogeneity at the interface will lead to a self-energy and ion-image interactions [27], we assume in this work that the carbon electrode and ionic liquids have similar dielectric constants such that the image charge effects are negligible. To further simplify our theoretical calculations, we fix the electrical potential at the surface such that the electric field inside the pore is exclusively determined by the ionic distributions, immaterial to the electronic properties of the electrode [28,29]. With the assumptions of uniform dielectric constant and constant surface electric potential, the self-energy and image forces are irrelevant for the DFT calculations.

From the ionic density profiles, we can readily calculate the ion adsorption from a bulk phase and related thermodynamic properties such as the capacitance. The charge density at the pore surface can be attained from the charge neutrality for the entire system

$$Q = -\frac{1}{2}\sum_i Z_i e\int_0^H dz\rho_i(z), \tag{4}$$

where the factor of ½ accounts for two surfaces of the slit pore. It is straightforward to show that charge neutrality in a slit pore is consistent with the prediction of Gauss's law.

III. RESULTS AND DISCUSSION

We consider first the ion partitioning between a bulk RTIL and a slit pore of zero electrical potential. While our coarse-gained model describes the ion size and interactions among EMIm, TFSI, and BF_4 in the mixture only approximately, in the following, we designate EMIm as cations, and TFSI and BF_4 as the large and the small anions, respectively, for the convenience of discussion. The physics is generically applicable to pore selectivity and partitioning for all ionic mixtures.

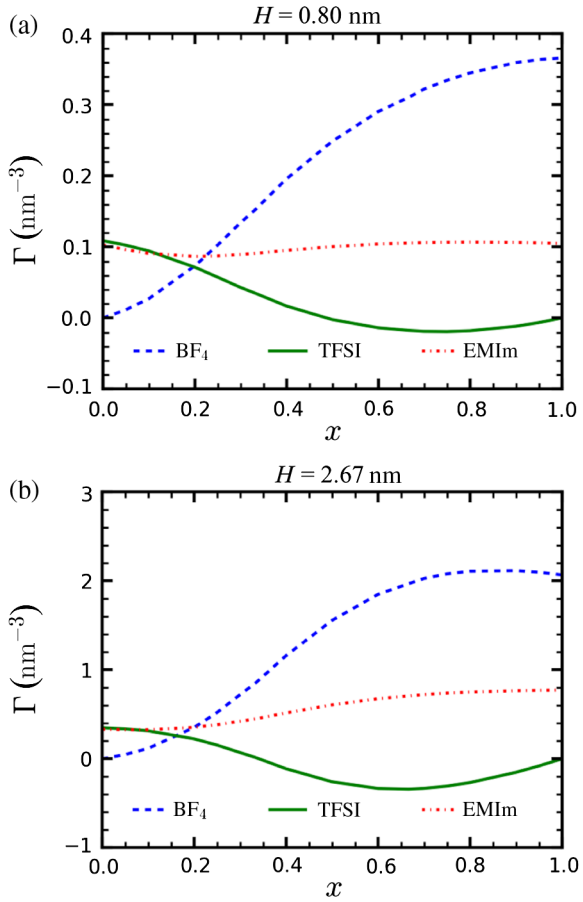

FIG. 2. Excess absorption (Γ) in a slit pore of zero electric potential versus the BF_4 mole fraction (x) in the bulk for an ionic liquid mixture consisting of EMIm, TFSI, and BF_4. (a) The pore width is $H = 0.8$ nm and (b) $H = 2.67$ nm.

Figure 2 presents the DFT predictions for the adsorption of different ionic species by two slit pores as a function of the mole fraction of BF_4 (x) in the bulk phase. Here, the excess absorption for individual ions is defined as

$$\Gamma_i = \frac{1}{H}\int_0^H [\rho_i(z) - \rho_i^0]dz \equiv \bar{\rho}_i - \rho_i^0, \tag{5}$$

where $\bar{\rho}_i$ stands for the average density of ion i inside the pore. In the absence of BF_4 ($x = 0$), the ionic liquid is composed of symmetric anions and cations. In this case, the system is everywhere neutral as cations and anions have the same density profile. As a result, the ion partitioning behavior is similar to that for neutral particles (*viz.*, ion pairs), which favors particle accumulation inside the pore due to the excluded volume effects.

Figure 2 indicates that the ionic liquid is slightly enriched inside the pore even without the surface attraction. The enrichment of cations and anions in the neutral pore can be attributed to the molecular exclusion effect for the ionic pairs, similar to that for the partitioning of neutral particles [30,31]. We note in passing that ionic liquid

partitioning into a neutral pore is qualitatively different from that for an aqueous electrolyte solution [14]. In the latter case, the ionic behavior inside the pore is determined not only by its size and valence but, more important, also by ion dehydration and solvent-wetting behavior of the solid surface [12]. Because of the hydration effects, an aqueous electrolyte is typically excluded from a neutral pore [32]. Figure 2 shows that the excess adsorption becomes more significant as the pore size increases because the average density inside the pore is defined over the entire space. In a larger pore, the "dead volume," i.e., the space not accessible to ionic species, makes less contribution to the average density.

Ion partitioning into a neutral pore is enhanced if cations and anions are asymmetric. For the two slit pores in contact with EMIm and BF_4 ($x = 1$) as shown in Fig. 2, BF_4 is more favored inside the pore in comparison to EMIm regardless of the pore width. The enrichment of small anions is in agreement with higher capacitance values observed experimentally for BF_4, which is also the reason for the widespread use of the BF_4 cations in organic electrolytes for supercapacitor applications [1]. Because the surface electric potential is fixed at zero in our DFT calculations, the slit pore becomes positively charged in the presence of an asymmetric ionic liquid. As discussed before for ion partitioning between a slit pore and ions in an aqueous solution [13,33], the positive charge at the surface is responsible for the stronger adsorption of the smaller counterions inside the pore.

When a slit pore of zero electric potential at the surface is in contact with an ionic liquid mixture containing two anions of the same valence but different sizes, DFT predicts that cation adsorption is relatively insensitive to the bulk composition. As shown in Fig. 2, the excess adsorption for the small anions BF_4 increases with its bulk composition. While the dependence of BF_4 adsorption on its bulk density is monotonic for the small pore ($H = 0.8$ nm), we see a maximum for BF_4 adsorption in the large pore ($H = 2.67$ nm). The nonmonotonic behavior reflects the competing effects of molecular-excluded volume, electrostatic correlations, and the entropy of mixing. Because of the induced surface charge, the electrostatic energy favors BF_4 enrichment against both EMIm and TFSI ions. At high BF_4 concentrations, however, both the ionic size and the mixing entropy effects are against further repulsion of TFSI and BF_4 accumulation. Such competing effects are also evident from the variation of the excess adsorption for the large anions, TFSI. Regardless of the pore size, the TFSI adsorption falls initially as the BF_4 mole fraction in the bulk increases, while the trend is reversed at high BF_4 concentrations.

Why does a slit pore at the zero electrical potential attract small ions significantly stronger than large ions? If all ions are neutral, a slit pore will adsorb more large ions due to the entropic effects [30,31]. In the presence of the electrostatic

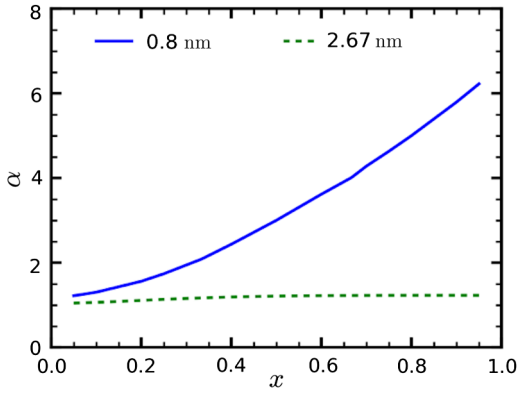

FIG. 3. Ion selectivity coefficient (α) for a slit pore of zero electric potential as a function of the BF_4 mole fraction (x) in the bulk. The legends denote the slit-pore width $H = 0.8$ and 2.67 nm.

interactions, however, any preferential adsorption of cations or anions breaks down the charge neutrality, inducing a net charge at the surface. Because the electrostatic energy is inversely proportional to the ionic radius for ions in direct contact with the surface, minimization of the electrical energy leads to the preferential adsorption of small ions. Although ion adsorption in charged nanopores has been reported before (e.g., by Hou *et al.* [13] and by Valisko *et al.* [33]), we are unaware of previous studies of similar effects introduced by the induced surface charge due to the size or valence asymmetry between cations and anions.

Figure 3 shows the effects of the pore size and the bulk ionic composition on the selectivity of two anions with different diameters. As usual, the selectivity coefficient is defined as

$$\alpha \equiv \frac{\bar{\rho}_{BF_4}}{\bar{\rho}_{TFSI}} \cdot \frac{\rho^0_{TFSI}}{\rho^0_{BF_4}}. \tag{6}$$

DFT predicts that for both pores, the ion selectivity rises monotonically as the BF_4 concentration in the bulk increases. The increase in the selectivity coefficient is nearly exponential in the small pore, suggesting that adsorption of small ions is self-amplified; i.e., the higher BF_4 density inside the pore, the higher charge density at the surface, and the more selective is the slit pore for small ions.

The self-amplified effect on the adsorption of small ions is also evident from the rapid rise of the surface charge density as the BF_4 concentration increases. Although the surface electrical potential is set at zero, a positive charge emerges at the electrode surface due to the asymmetric distributions of the cations and the anions inside the pore. Interestingly, as shown in Fig. 4, the surface charge density for the 0.8-nm pore is close to that of the 2.675-nm pore. The apparent insensitivity of the induced surface charge and the pore width reflects the oscillatory distribution of ionic species in small pores. We find that, in general, the

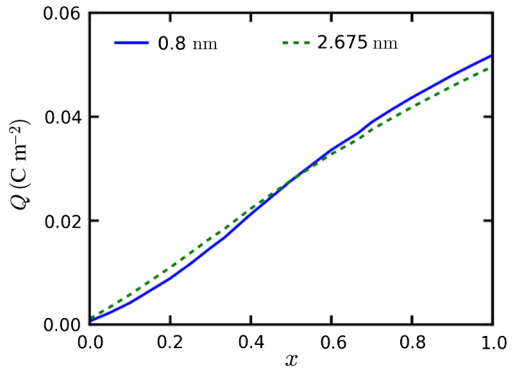

FIG. 4. The surface charge density (Q) for a slit pore of zero electric potential in contact mixed RTILs containing EMIm, TFSI, and BF_4. The legends represent pore width $H = 0.8$ and 2.67 nm, and x is the BF_4 mole fraction in the bulk.

surface charge density shows an oscillatory dependence on the pore size, similar to what is observed for the capacitance [24,34,35].

We may understand the exponential increase of the selectivity based on the ionic density profiles. According to Eqs. (2) and (6), the selectivity coefficient can be written as

$$\alpha = \frac{\int dz \exp[-\beta V_{BF_4}(z) + \beta e\psi(z) - \beta\Delta\mu^{ex}_{BF_4}(z)]}{\int dz \exp[-\beta V_{TFSI}(z) - \beta e\psi(z) - \beta\Delta\mu^{ex}_{TFSI}(z)]}$$
$$\approx \frac{H_{BF_4}}{H_{TFSI}} \frac{\exp(-\beta\overline{\Delta\mu^{ex}_{BF_4}})}{\exp(-\beta\overline{\Delta\mu^{ex}_{TFSI}})} \exp(2\beta e\bar{\psi}), \quad (7)$$

where $H_i = H - \sigma_i$ stands for the pore width accessible to the confined ion of type i, $\overline{\Delta\mu_i^{ex}}$ represents the average excess chemical potential for ion i inside the pore relative to its bulk value, and $\bar{\psi}$ is the mean electrical potential inside the pore. On the one hand, Eq. (7) indicates that the selectivity for small ions increases as the pore size falls, as shown correctly in Fig. 3, and it approaches infinity when the pore size is the same as the TFSI diameter ($H_{TFSI} = 0$). On the other hand, the excess chemical potential includes contributions from both excluded volume effects and ion correlations. Approximately, this term reflects the average insertion work for the ionic species and can be related to the normal pressure inside the pore and the particle volume. Because the normal pressure is a quadratic function of the surface charge density [36] and the mean electrical potential inside the pore is linearly related to the surface charge, the positive correlation between the surface charge and counterion concentration shown in Fig. 4 implies an exponential increase of the selectivity with the BF_4 mole fraction.

The ion distribution in an ionic liquid is fundamentally different from that in an aqueous electrolyte solution. As indicated in previous experimental and theoretical studies [23,37,38], RTILs may exhibit alternating distributions of

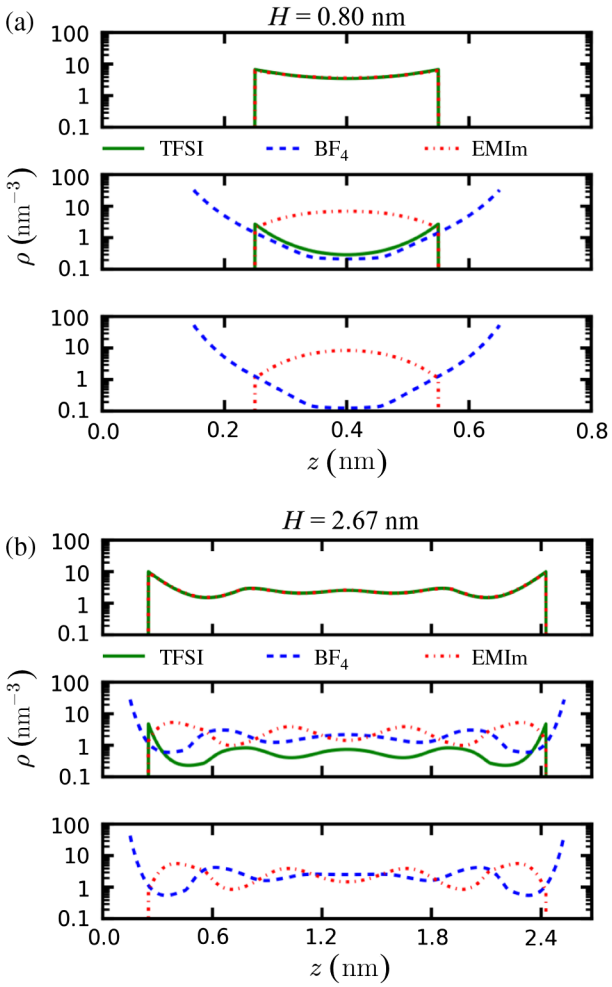

FIG. 5. The density profiles of cations and anions across the pore at three representative BF_4 mole fractions (x) in the bulk. (a) The pore width is $H = 0.8$ nm, and from top to bottom, $x = 0.0$, 0.67, and 1.0. (b) The pore width is $H = 2.67$ nm, and from top to bottom, $x = 0.0$, 0.75, and 1.0.

cations and anions near a solid surface. The layering structure can be attributed to charge inversion, i.e., oscillatory sign variation in the local charge density. Figure 5 shows that in a large pore ($H = 2.67$ nm), the oscillatory distributions of ionic species are evident in both symmetric and asymmetric ionic liquids as well as in the mixtures. In a small pore ($H = 0.8$ nm), however, the local ion densities change monotonically from the surface and show a minimum for the anions and maximum for the cation at the center. The multilayer structure is suppressed due to the strong confinement, and the small pore size is also responsible for the deficit of cations inside the pore. Because charge neutrality must be satisfied for the entire cell, the unbalanced partitioning of cations and anions in the pore generates the induced charge at the electrode surface.

Our coarse-grained model accounts for ionic size and electrostatic interactions among all ionic species explicitly

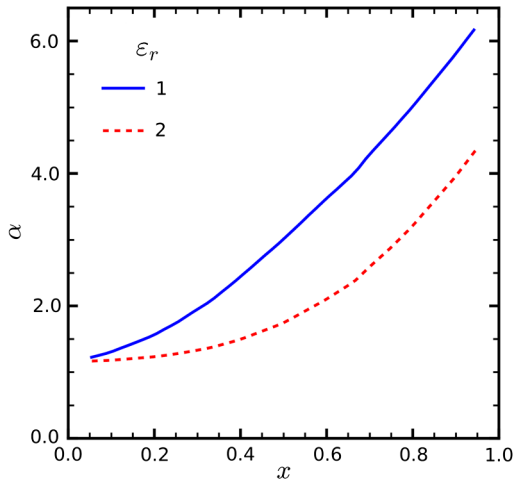

FIG. 6. The effect of residue dielectric constant (ε_r) on ion selectivity coefficient (α) for a narrow ($H = 0.8$ nm) slit pore of zero electric potential as a function of the BF_4 mole fraction (x) in the bulk.

but ignores polarizability effects. Ionic polarization may contribute to an effective dielectric constant that reduces the magnitude of electrostatic interactions. While an accurate assessment of the "residual" dielectric constant is beyond the scope of this work, we consider its influence on ion selectivity by the narrow pore ($H = 0.8$ nm). As shown in Fig. 6, the ion selectivity is noticeably reduced as the dielectric constant increases, indicating that the self-charging effect will be less significant. It should be noted that the dielectric constant of an ionic liquid in a narrow pore is different from the bulk value even in the presence of a solvent. In the presence of solvent molecules, one must consider their excluded volume effects and ion desolvation in addition to dielectric screening. For ionic liquid systems considered in this work, it is clear that ion polarizability does not change the qualitative picture.

IV. CONCLUSION

A charged pore enriches counterions over coions due to the electrostatic attraction, and, in the presence of two kinds of counterions of the same valence, it favors smaller counterions due to the stronger contact energy. While the preferential adsorption of counterions has been reported before for aqueous systems, we find in this work that for nanopores in contact with a mixed room-temperature ionic liquid, the selective adsorption of smaller ions can be similarly achieved with the induced charge, i.e., a net charge introduced on the surface to ensure the zero electrical potential. The surface charge is nonzero due to the uneven distribution of cations and anions. In other words, the asymmetry in ionic size leads to preferential adsorption of small ions and the subsequent development of a net surface charge that promotes further enrichment of the small ions. The self-amplified surface charging and preferential adsorption of small ions in a neutral pore is less likely to occur for aqueous systems. It is our hope that the unique features of room-temperature ionic liquids in nanopores will open up new directions of research for strongly correlated inhomogeneous electrolyte systems. From a practical perspective, the self-amplified ion partitioning and surface charging have clear implications for supercapacitor design and may be utilized for other practical applications including ion separation and harvesting renewable energy. Work along those directions is under way and will be published in the future.

ACKNOWLEDGMENTS

This research is sponsored by the Fluid Interface Reactions, Structures and Transport Center, an Energy Frontier Research Center funded by the U.S. Department of Energy, Office of Science, Office of Basic Energy Sciences. The numerical calculations are performed at the National Energy Research Scientific Computing Center.

[1] P. Simon and Y. Gogotsi, Capacitive energy storage in nanostructured carbon-electrolyte systems, Acc. Chem. Res. **46**, 1094 (2013).
[2] M. Kar, T. J. Simons, M. Forsyth, and D. R. MacFarlane, Ionic liquid electrolytes as a platform for rechargeable metal-air batteries: A perspective, Phys. Chem. Chem. Phys. **16**, 18658 (2014).
[3] M. Armand, F. Endres, D. R. MacFarlane, H. Ohno, and B. Scrosati, Ionic-liquid materials for the electrochemical challenges of the future, Nat. Mater. **8**, 621 (2009).
[4] J. Vatamanu, Z. Z. Hu, D. Bedrov, C. Perez, and Y. Gogotsi, Increasing energy storage in electrochemical capacitors with ionic liquid electrolytes and nanostructured carbon electrodes, J. Phys. Chem. Lett. **4**, 2829 (2013).
[5] C. Merlet, B. Rotenberg, P. A. Madden, P. L. Taberna, P. Simon, Y. Gogotsi, and M. Salanne, On the molecular origin of supercapacitance in nanoporous carbon electrodes, Nat. Mater. **11**, 306 (2012).
[6] A. A. Lee, S. Kondrat, D. Vella, and A. Goriely, Dynamics of Ion Transport in Ionic Liquids, Phys. Rev. Lett. **115**, 106101 (2015).
[7] Z. Li, O. Borodin, G. D. Smith, and D. Bedrov, Effect of organic solvents on Li+ ion solvation and transport in ionic liquid electrolytes: A molecular dynamics simulation study, J. Phys. Chem. B **119**, 3085 (2015).
[8] A. Balducci, R. Dugas, P. L. Taberna, P. Simon, D. Plee, M. Mastragostino, and S. Passerini, High temperature carbon-carbon supercapacitor using ionic liquid as electrolyte, J. Power Sources **165**, 922 (2007).
[9] W. Y. Tsai, R. Y. Lin, S. Murali, L. L. Zhang, J. K. McDonough, R. S. Ruoff, P. L. Taberna, Y. Gogotsi, and P. Simon, Outstanding performance of activated graphene based supercapacitors in ionic liquid electrolyte from -50 to 80°C, Nano Energy **2**, 403 (2013).

[10] M. LozadaCassou, W. Olivares, and B. Sulbaran, Violation of the electroneutrality condition in confined charged fluids, Phys. Rev. E **53**, 522 (1996).
[11] Y. Gogotsi, Not just graphene: The wonderful world of carbon and related nanomaterials, MRS Bull. **40**, 1110 (2015).
[12] R. Roth and D. Gillespie, Physics of Size Selectivity, Phys. Rev. Lett. **95**, 247801 (2005).
[13] C. H. Hou, P. Taboada-Serrano, S. Yiacoumi, and C. Tsouris, Electrosorption selectivity of ions from mixtures of electrolytes inside nanopores, J. Chem. Phys. **129**, 224703 (2008).
[14] R. K. Kalluri, T. A. Ho, J. Biener, M. M. Biener, and A. Striolo, Partition and structure of aqueous NaCl and $CaCl_2$ electrolytes in carbon-slit electrodes, J. Phys. Chem. C **117**, 13609 (2013).
[15] F. Moucka, D. Bratko, and A. Luzar, Electrolyte pore/solution partitioning by expanded grand canonical ensemble Monte Carlo simulation, J. Chem. Phys. **142**, 124705 (2015).
[16] L. Yang and S. Garde, Modeling the selective partitioning of cations into negatively charged nanopores in water, J. Chem. Phys. **126**, 084706 (2007).
[17] R. H. Nilson and S. K. Griffiths, Influence of atomistic physics on electro-osmotic flow: An analysis based on density functional theory, J. Chem. Phys. **125**, 164510 (2006).
[18] D. Gillespie, High energy conversion efficiency in nanofluidic channels, Nano Lett. **12**, 1410 (2012).
[19] K. L. Van Aken, M. Beidaghi, and Y. Gogotsi, Formulation of ionic-liquid electrolyte to expand the voltage window of supercapacitors, Angew. Chem., Int. Ed. Engl. **54**, 4806 (2015).
[20] H. S. Kim, J. P. Singer, Y. Gogotsi, and J. E. Fischer, Molybdenum carbide-derived carbon for hydrogen storage, Microporous Mesoporous Mater. **120**, 267 (2009).
[21] P. B. Balbuena and K. E. Gubbins, Theoretical interpretation of adsorption behavior of simple fluids in slit pores, Langmuir **9**, 1801 (1993).
[22] J. Hoffmann and D. Gillespie, Ion correlations in nanofluidic channels: Effects of ion size, valence, and concentration on voltage- and pressure-driven currents, Langmuir **29**, 1303 (2013).
[23] J. Wu, T. Jiang, D.-e. Jiang, Z. Jin, and D. Henderson, A classical density functional theory for interfacial layering of ionic liquids, Soft Matter **7**, 11222 (2011).
[24] D.-e. Jiang, Z. Jin, and J. Wu, Oscillation of capacitance inside nanopores, Nano Lett. **11**, 5373 (2011).
[25] J. Wu and Z. Li, Density-functional theory for complex fluids, Annu. Rev. Phys. Chem. **58**, 85 (2007).
[26] D.-e. Jiang, D. Meng, and J. Wu, Density functional theory for differential capacitance of planar electric double layers in ionic liquids, Chem. Phys. Lett. **504**, 153 (2011).
[27] Z. G. Wang, Fluctuation in electrolyte solutions: The self-energy, Phys. Rev. E **81**, 021501 (2010).
[28] S. Kondrat and A. Kornyshev, Superionic state in double-layer capacitors with nanoporous electrodes, J. Phys. Condens. Matter **23**, 022201 (2011).
[29] J. Comtet, A. Nigues, V. Kaiser, B. Coasne, L. Bocquet, and A. Siria, Nanoscale capillary freezing of ionic liquids confined between metallic interfaces and the role of electronic screening, Nat. Mater. **16**, 634 (2017).
[30] Y. X. Yu, J. Z. Wu, Y. X. Xin, and G. H. Gao, Structures and correlation functions of multicomponent and polydisperse hard-sphere mixtures from a density functional theory, J. Chem. Phys. **121**, 1535 (2004).
[31] Z. H. Jin, S. L. Zhao, and J. Z. Wu, Entropic forces of single-chain confinement in spherical cavities, Phys. Rev. E **82**, 041805 (2010).
[32] R. K. Kalluri, D. Konatham, and A. Striolo, Aqueous NaCl Solutions within charged carbon-slit pores: Partition coefficients and density distributions from molecular dynamics simulations, J. Phys. Chem. C **115**, 13786 (2011).
[33] M. Valisko, D. Boda, and D. Gillespie, Selective adsorption of ions with different diameter and valence at highly charged interfaces, J. Phys. Chem. C **111**, 15575 (2007).
[34] G. Feng and P. T. Cummings, Supercapacitor capacitance exhibits oscillatory behavior as a function of nanopore size, J. Phys. Chem. Lett. **2**, 2859 (2011).
[35] P. Wu, J. S. Huang, V. Meunier, B. G. Sumpter, and R. Qiao, Complex capacitance scaling in ionic liquids-filled nanopores, ACS Nano **5**, 9044 (2011).
[36] J. Jiang, D. P. Cao, D. Henderson, and J. Z. Wu, A contact-corrected density functional theory for electrolytes at an interface, Phys. Chem. Chem. Phys. **16**, 3934 (2014).
[37] M. Z. Bazant, B. D. Storey, and A. A. Kornyshev, Double Layer in Ionic Liquids: Overscreening versus Crowding, Phys. Rev. Lett. **106**, 046102 (2011).
[38] Y. Lauw, M. D. Horne, T. Rodopoulos, and F. A. M. Leermakers, Room-Temperature Ionic Liquids: Excluded Volume and Ion Polarizability Effects in the Electrical Double-Layer Structure and Capacitance, Phys. Rev. Lett. **103**, 117801 (2009).